Desalination and Water Treatment
www.deswater.com
doi: 10.5004/dwt.2019.23215

137 (2019) 279–291
January

Efficient and fast removal of nitrate from water using a novel lignocellulosic anion exchanger modified with a silane group

Leila Manhooei[a], Behrouz Mehdinejadiani[a,*], S. Mojtaba Amininasab[b]

[a]*Department of Water Science and Engineering, Faculty of Agriculture, University of Kurdistan, Sanandaj, Iran, Tel. +98-918-3708731; Fax: +98-873-3624004; emails: b.mehdinejad@uok.ac.ir (B. Mehdinejadiani), leila.manhooei70@gmail.com (L. Manhooei)*
[b]*Polymer Chemistry Research Laboratory, Department of Chemistry, Faculty of Science, University of Kurdistan, Sanandaj, Iran, email: m.amininasab@uok.ac.ir (S.M. Amininasab)*

Received 8 March 2018; Accepted 28 September 2018

ABSTRACT

A novel anion exchanger was prepared by modifying poplar sawdust (PSD) with 3-chloro propyl trimethoxysilane and (1,4-diazabicyclo[2.2.2]octane). After characterizing the physicochemical properties of PSD and modified PSD (MPSD), the effects of various operational conditions on nitrate adsorption by MPSD were examined. The results indicated that the MPSD removed over 98% of nitrate from water at optimum operation conditions, i.e. C_i = 20 mg L^{-1}; pH_i = 7; T = 25 ± 1°C; adsorbent dosage = 2 g L^{-1}; and contact time = 30 min. Kinetic studies showed that the adsorption process followed the pseudo-second-order model and was a three-step process. Among the equilibrium isotherms, Freundlich model provided the best fit to the experimental data, which demonstrated multilayer adsorption of nitrate on heterogeneous surfaces. According to thermodynamic studies, the nitrate adsorption by MPSD was exothermic ($\Delta H° < 0$) and spontaneous ($\Delta G° < 0$) in nature. Among the studied competing anions, sulfate had the maximum inhibition effect on the nitrate adsorption by MPSD, while phosphate had the minimum effect. In a nutshell, it can be concluded from the experimental results that the MPSD was an efficient and economical adsorbent for nitrate removal from water.

Keywords: Anion exchange; Competing anions; Lignocellulosic materials; Multilayer adsorption; Nitrate-contaminated water

1. Introduction

In recent years, due to the fast development of agricultural and industrial activities, concentrations of various pollutants such as persistent organic pollutants (e.g., perfluoroalkyl substances, dichlorodiphenyltrichloroethanes, and hexabromocyclododecanes) [1], chemical fertilizers (e.g., nitrogen, phosphorus, and potassium), pesticides [2], and industrial pollutants (e.g., dyes, surfactants, caustic compounds, scouring agents, metal ions, phenols, bleaches, xylenes, and acids) [3] have increased in water resources. Among the various pollutants, nitrate is one of the most incident ones, which has been reported in many water resources [4]. In most cases, this pollution results from anthropogenic activities including intense agriculture and urbanization [5,6]. The nitrate pollution of drinking water resources can potentially cause the incidence of various diseases such as methemoglobinemia in infants, colorectal cancer, gastric cancer, cyanosis, cancer of alimentary, and non-Hodgkin lymphoma in adults [7,8]. Because of the health risk of excessive nitrate in water, the nitrate concentration in the drinking water should be below 50 mg L^{-1} based on the World Health Organization standard [9]. Therefore, if nitrate concentration in water exceeds the mentioned values at various standards, it will be necessary to remove it from water and keep the concentration below the allowable threshold. Excessive nitrate can be removed from water using biological denitrification [10], reverse osmosis [11], electrodialysis and electrodeionization [12],

* Corresponding author.

adsorption [13], and chemical reduction [14]. Among these methods, the adsorption technique is generally considered to be the most attractive method because of its efficiency, ease of operation, simplicity of design, and cost effectiveness [15,16].

Several natural and synthetic materials including anion exchange resins, agricultural wastes, zeolite, fly ash, and red mud were used as adsorbents to remove nitrate from water [17]. Among the mentioned materials, anion exchange resins are one of the most promising adsorbents to remove nitrate from water [5,17,18]. In recent years, different types of commercial anion exchange resins such as Purolite A520E [7], IRA-400 [19], and Indion NSSR [20] have been used to remove nitrate from water. The major drawback of commercial anion exchange resins is their high cost [21]. Hence, the application of cheap lignocellulosic materials to treat contaminated waters has been of great interest in the past decades [e.g., 21–25]. These materials with their many reactive functional groups provide a bio-based platform to produce anion exchange materials [24]. Chemical modification is required to enhance the anion exchange properties of lignocellulosic materials [21,24]. The chemical modification, which includes cross-linking and introducing various amine groups into lignocellulosic structure [24], is commonly carried out by using epichlorohydrin, dimethylamine, ethylenediamine, and trimethylamine in the presence of *N*,*N*-dimethylformamide [22,24–27]. The main drawback of the above chemical modification process is the high toxicity of epichlorohydrin [28]. This has increased the interest to make use of less hazardous solvent or reagents, which is called green chemistry. Abbott et al. [29] demonstrated the efficient cationic functionalization of cotton wool using an ionic liquid analogue based on a eutectic mixture of a choline chloride derivative and urea. The coconut shell fiber, which was modified with *N*-(3-chloro-2-hydroxypropyl) trimethylammonium chloride (CHMAC) in the presence of sodium hydroxide (NaOH) [30], removed nitrate up to 33.7 mg g^{-1}. Karachalios and Wazne [21] used an ionic liquid analogue comprised of a choline chloride derivative and urea to modify pine bark (PB). The modified PB had a maximum nitrate adsorption capacity of 180.42 mg g^{-1}. The anion exchange property of pine sawdust was increased using CHMAC in the presence of NaOH [24]. The maximum nitrate sorption capacity of 67.76 ± 6.20 mg g^{-1} was reported for the modified pine sawdust. Mautner et al. [31] produced a nanopaper ion-exchanger using cellulose nanofibrils modified with glycidyltrimethylammonium chloride in the presence of NaOH. The maximum nitrate sorption capacity of 12 mg g^{-1} was achieved by the nanopaper. A commercial granular activated carbon (AC) was treated with cetyl trimethyl ammonium bromide in the presence of NaOH [8]. According to the results of this study, the modified AC improved the nitrate removal efficiency significantly.

In recent years, the application of silane groups has increased to remove contaminants from water [e.g., 32]. However, to the authors' knowledge, these groups have not yet been used to modify lignocellulosic materials and remove nitrate from water. Therefore, the objectives of this study were to (1) modify and characterize a poplar sawdust (PSD) as a lignocellulosic material, using 3-chloro propyl trimethoxysilane and (1,4-diazabicyclo[2.2.2]octane) (Dabco); (2) investigate the effects of solution pH, contact time, initial concentration of nitrate, adsorbent dosage, temperature, and competing anions on the nitrate adsorption capacity by modified PSD (MPSD); and (3) fit the experimental data to different adsorption kinetic and isotherm models for determining the best kinetic and isotherm models.

2. Materials and methods

2.1. Materials and reagents

PSD used in this study was obtained from a local forest in Sari, Iran. 3-chloro propyl trimethoxysilane, Dabco, toluene, potassium nitrate (KNO_3), hydrochloric acid (HCl), NaOH, ammonium chloride (NH_4Cl), potassium dihydrogen phosphate (KH_2PO_4), sodium hydrogen carbonate ($NaHCO_3$), and magnesium sulfate ($MgSO_4$) were purchased from Merck (Germany). All the chemicals were of reagent grade and used without any further purification.

2.2. Modification of PSD

The synthesis process for adsorbent was divided into two steps. The silanated intermediate was synthesized in the first step by nucleophilic substitution reaction between amine and alkyl halide groups, in which an aliquot of 0.56 g (5 mmol) of Dabco was reacted with 1.82 mL (10 mmol) of 3-chloro propyl trimethoxysilane in 10 mL of toluene solvent at 80°C under N_2 atmosphere. After stirring for 12 h, the intermediate was collected and used in the following reactions. The MPSD was produced in the second step of the synthesis process. In this step, a condensation reaction between hydroxyl groups of PSD and methoxysilane occurred as follows: 2 g of PSD was reacted with 2 g of intermediate and 10 mL acetic acid/ethanol solution (1:9 V/V) in a 100-mL two-neck round-bottom flask for 12 h at 80°C. The product was washed with 100 mL of ethanol/distilled water (50:50 V/V) to remove the residual chemicals, dried at 60°C for 12 h, and sieved to obtain particles smaller than 210 μm in diameter and then used in all the adsorption experiments. The synthesis process of MPSD is presented in Fig. 1.

2.3. Instrumentation and characterizations of PSD and MPSD

The size and morphology of PSD, MPSD, and MPSD-loaded nitrate were characterized by Field Emission Scanning Electron Micrographs (FESEM) using a Mighty-8 instrument (TSCAN Company, Prague). Also, scanning electron microscopy–energy dispersive spectroscopy (SEM–EDS) and elemental mapping images were acquired using Mighty-8 instrument (TSCAN Company, Prague). Specific surface area and pore size diameter of MPSD were determined from nitrogen adsorption isotherms by using Brunauer, Emmett, and Teller (BET) method. Thermogravimetric analysis (TGA) was performed by a DuPont Instruments TGA 951 from room temperature to 700°C with a heating rate of 10°C min^{-1} in a nitrogen flow. Fourier transform infrared (FT-IR) spectra of PSD and MPSD were recorded with Bruker Tensor 27 spectrometer using KBr method. The nitrate ion concentration in the solutions was detected by a UV-vis spectrophotometer (SPECORD 210 Plus, Analytic Jena, Germany).

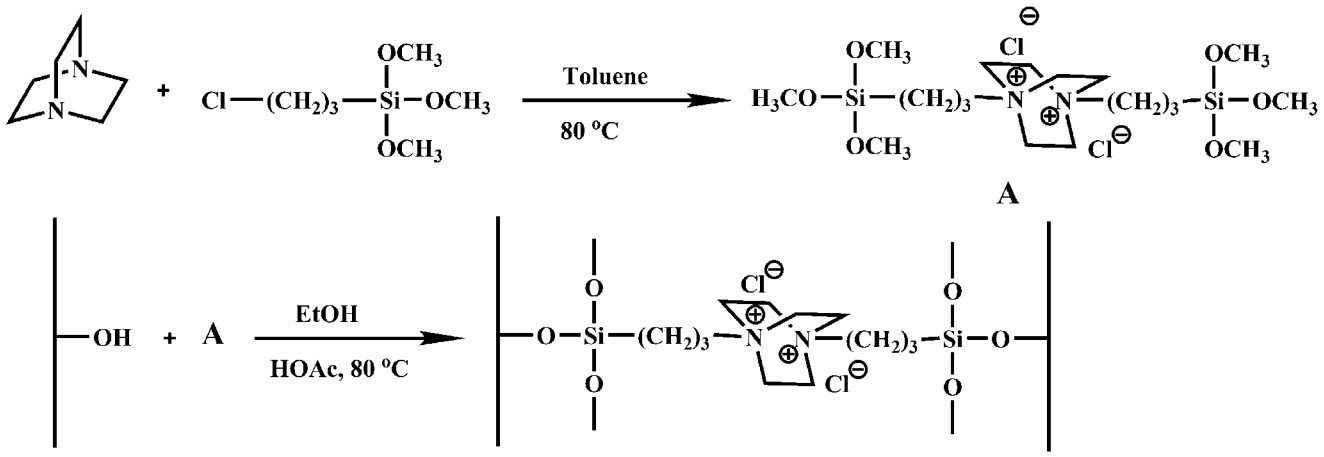

Fig. 1. Illustration of synthesis procedure of MPSD.

2.4. Batch adsorption studies

The batch adsorption experiments were conducted to examine the effect of experimental conditions on nitrate removal from water using MPSD. The preliminary experiment showed less favorability of PSD in removing nitrate from water. Therefore, the batch adsorption experiments were only performed with the MPSD. The batch adsorption experiments were performed with 20 mL of nitrate solution in a volumetric flask. Required different concentrations of nitrate solutions in batch experiments were obtained by serial dilution of the stock solution. After adding a predetermined amount of MPSD to nitrate solution, the mixture was continuously stirred using a magnetic mixer (IKA RH basic2, Germany) at 120 rpm for desired pH, contact time, and temperature. Afterward, the sample was filtered through a Whatman 42 filter paper. Finally, the residual nitrate concentration in the filtered sample was measured using the spectrophotometer. According to Zhang et al. [33], the nitrate concentration was calculated by measuring ultraviolet absorbance at 220 nm and corrected by subtracting a second absorbance at 275 nm. All the experiments were conducted at room temperature (25°C ± 1°C) except for the ones operated at different temperatures to study the temperature effects. Each experiment was triplicated to ensure the reproducibility of the measurements, and the reported result was the average of three repetitions. In all the batch adsorption experiments, the efficiency of nitrate removal, E (%), and the adsorption capacity at any time t, q_t (mg g^{-1}), were calculated using the following equations:

$$E(\%) = \frac{C_i - C_t}{C_i} \times 100 \quad (1)$$

$$q_t = \frac{C_i - C_t}{m} \times V \quad (2)$$

where C_i is the initial nitrate concentration (mg L^{-1}), C_t is the nitrate concentration at time t (mg L^{-1}), V is the solution volume (L), and m is the adsorption mass (g). Details of batch adsorption experiments including the effects of initial solution pH, contact time, adsorbent dosage, initial nitrate concentration, temperature, and competing anions are described in the subsequent subsections.

2.4.1. Effect of initial solution pH

The solution pH is an important controlling parameter in all the adsorption processes, which significantly influences surface charge and ionization degree of adsorbent as well as dissociation of adsorbent functional groups [26]. To study the effect of pH, the initial pH of the nitrate solution samples (20 mL, 20 mg L^{-1}) was adjusted to 3–11 using 0.1 M HCl and 0.1 M NaOH. The pH values of the samples were measured by a pH meter (Inolab pH 7110, WTW, Weilheim, Germany). Then, 0.04 g of MPSD (2 g L^{-1}) was added to each sample and stirred for 2 h. Finally, the samples were filtered and the residual nitrate concentrations measured.

2.4.2. Effect of contact time

The contact time between adsorbent and solution is an important factor from a process design viewpoint because it affects the pollutant diffusion onto the adsorption surface and the reaction with functional groups [24]. The effect of contact time was investigated by adding 0.04 g of MPSD (2 g L^{-1}) to the nitrate solution samples (20 mL, 20 mg L^{-1}) under the optimal initial pH (pH$_i$ = 7) and stirring the samples for predetermined contact times (5, 10, 20, 30, 45, 60, 90, and 120 min). At the end of the different stirring periods, the samples were filtered and analyzed for residual nitrate concentration.

2.4.3. Effect of adsorbent dosage

Adsorbent dosage is a vital factor to be considered for an effective and economical removal [34]. In general, the efficiency of removal enhances with increasing the adsorbent dosage, which is typically attributed to the greater surface area and the availability of more active adsorption sites [26]. In this work, to study the effect of adsorbent dosage, different amounts of MPSD (0.25, 0.50, 1, 1.50, and 2 g L^{-1}) were added to 20 mL of nitrate solution (20 mg L^{-1}) at optimal initial pH (pH$_i$ = 7). The samples were stirred for 30 min

(equilibrium contact time) and filtered, and the residual nitrate concentrations were measured.

2.4.4. Effect of initial nitrate concentration

The effect of initial nitrate concentration was examined by adding the optimum adsorbent dosage of 2 g L^{-1} to 20 mL of the nitrate solution samples with different initial concentrations of 20, 40, 60, 80, 100, and 150 mg L^{-1}. The pH values of samples were adjusted to the optimum initial pH (pH_i = 7) prior to the addition of adsorbent. The samples were stirred for 30 min (equilibrium contact time). At the end of each experiment, the solid phase was separated from the solution by filtration and the residual nitrate concentration in the filtered solution was measured.

2.4.5. Kinetic adsorption models

The kinetic studies are of great importance from practical viewpoint because they provide useful information for economic and efficient design, operation, and control of system [35]. To investigate the mechanism of adsorption, the studies of adsorption kinetics were carried out using pseudo-first-order (PFO) kinetic model, pseudo-second-order (PSO) kinetic model, and Elovich kinetic model. The nonlinear forms of PFO and PSO kinetic models are given as follows [36]:

$$\text{PFO kinetic model: } q_t = q_e\left(1-\exp\left(-k_1 t\right)\right) \tag{3}$$

$$\text{PSO kinetic model: } q_t = \frac{k_2 q_e^2 t}{1+k_2 q_e t} \tag{4}$$

$$\text{Elovich model: } q_t = \frac{1}{\beta}\ln\left(1+\alpha\beta t\right) \tag{5}$$

where q_t and q_e are the adsorption capacities (mg g^{-1}) at a given time t and at equilibrium time e, respectively; t is the contact time (min); k_1 (min^{-1}), k_2 (g mg^{-1} min^{-1}), α (mg g^{-1} min^{-1}), and β (g mg^{-1}) are the constants of PFO, PSO, and Elovich models, respectively. The parameters of PSO (k_2 and q_e) are applied to calculate the initial adsorption rate, h (mg g^{-1} min^{-1}), and half-adsorption time, $t_{1/2}$ (min), as follows [37]:

$$h = k_2 q_e^2 \tag{6}$$

$$t_{1/2} = \frac{1}{k_2 q_e} \tag{7}$$

Note that $t_{1/2}$ is the time required for reaching the half of adsorption capacity at equilibrium [37]. The parameters of kinetic adsorption models were calculated using "***Solver add-in***" in Microsoft Office Excel (2016 version), a nonlinear method recommended by many researchers [36,38,39]. In addition, the best-fit model was determined by calculating an error function, F_{error} (%), and determination coefficient, R^2, defined as follows [40]:

$$F_{error}(\%) = 100\times\sqrt{\frac{1}{n-p}\times\sum_{i=1}^{n}\left(\frac{q_{i,\exp}-q_{i,\text{model}}}{q_{i,\exp}}\right)^2} \tag{8}$$

$$R^2 = \frac{\sum_{i=1}^{n}\left(q_{i,\exp}-\bar{q}_{\exp}\right)^2-\sum_{i=1}^{n}\left(q_{i,\exp}-q_{i,\text{model}}\right)^2}{\sum_{i=1}^{n}\left(q_{i,\exp}-\bar{q}_{\exp}\right)^2} \tag{9}$$

where $q_{i,\exp}$ is each value of q experimentally measured; $q_{i,\text{mode}}$ is each value of q obtained from the fitted model; $\bar{q}_{\exp}$ is the average of the measured values of q; n is the number of measurement points; and p is the number of fitted model parameters. To compare various models, it is recommended that the F_{error} of each model is divided by the minimum of the obtained F_{error} value (F_{error} ratio) [40]. It should be noted that the model with the value of F_{error} ratio close to zero and R^2 close to unity is the best-fit model [40].

Also, the limiting step of the adsorption process was identified using intraparticle diffusion (IPD) model defined as follows [41]:

$$q_t = k_p\sqrt{t} + I \tag{10}$$

where k_p (mg g^{-1} $min^{-0.5}$) is the rate constant of the IPD model and I (mg g^{-1}) is a constant related to the thickness of the boundary layer. The larger value of I indicates the greater effect of the boundary layer on the adsorption process [36]. The parameters of the IPD model were calculated using a plot of q_t versus square root of contact time [8].

2.4.6. Equilibrium adsorption models

Adsorption isotherms describe the relationship between the concentration of adsorbate in the solution and the amount of adsorbate adsorbed by the adsorbent at a constant temperature when the adsorption process reaches an equilibrium state [36]. Several adsorption isotherm models have been applied to describe adsorption isotherm experimental data in the literature. In this study, the adsorption isotherm experimental data were analyzed using three widely used models, Langmuir, Freundlich, and Redlich–Peterson isotherm models. The nonlinear forms of these isotherms are expressed as follows [36]:

$$\text{Langmuir isotherm: } q_e = \frac{q_{\max}K_L C_e}{1+K_L C_e} \tag{11}$$

$$\text{Freundlich isotherm: } q_e = K_F C_e^{1/n_F} \tag{12}$$

$$\text{Redlich-Peterson isotherm: } q_e = \frac{K_{RP}C_e}{1+a_{RP}C_e^g} \text{ where } 0<g\le 1 \tag{13}$$

where $q_{\max}$ is the maximum adsorption capacity of adsorbent (mg g^{-1}); C_e is the residual nitrate concentration (mg L^{-1}) at equilibrium; K_L (L mg^{-1}), K_F (mg g^{-1} (mg $L^{-1})^{-1/n}$), and K_{RP} (L g^{-1}) and a_{RP} (mg $L^{-1})^{-g}$ are the constants of Langmuir, Freundlich, and Redlich–Peterson isotherms, respectively; n_F (dimensionless) and g (dimensionless) are, respectively, the exponents of Freundlich and Redlich–Peterson isotherms; and all other variables are defined as before.

Like the kinetic models, the parameters of adsorption isotherms were also obtained using "***Solver add-in***" in Microsoft

Office Excel (2016 version). The F_{error} and the adjusted form of R^2, R^2_{adj}, were employed to determine the best-fit equilibrium model. The F_{error} was calculated using Eq. (8) and the R^2_{adj} was obtained using the following equation [39]:

$$R^2_{adj} = 1 - \left(1 - R^2\right) \times \frac{n-1}{n-p-1} \tag{14}$$

where R^2 is calculated using Eq. (9) and all other variables are defined as before. It is necessary to mention here that the R^2_{adj} is an indicator to compare the models with different number of parameters [39]. Similarly, the value of F_{error} ratio was also calculated to compare the various adsorption isotherms.

2.4.7. Effect of temperature and thermodynamic studies

Thermodynamic analysis is essential to evaluate the feasibility and nature of adsorption process [8]. The thermodynamic nature of adsorption process by MPSD was examined by conducting the batch adsorption experiments at three different temperatures (room temperature (25°C ± 1°C), 35°C, and 45°C). To this end, the optimum adsorbent dosage (2 g L^{-1}) was mixed with 20 mL of the nitrate solution (20 mg L^{-1}) under the optimal initial pH (pH_i = 7). The mixture was stirred at the desired temperatures for 30 min (equilibrium contact time). Then, the samples were filtered and the residual nitrate concentrations were measured. Thermodynamic parameters including Gibbs free energy change, $\Delta G°$, enthalpy change, $\Delta H°$, and entropy change, $\Delta S°$, were calculated using the following equations [42]:

$$\mathrm{Log}\left(1{,}000\frac{q_e}{C_e}\right) = \frac{\Delta S^\circ}{2.303R} - \frac{\Delta H^\circ}{2.303RT} \tag{15}$$

$$\Delta G^\circ = \Delta H^\circ - T\Delta S^\circ \tag{16}$$

where R is the universal gas constant (8.314 J mol^{-1} K^{-1}), T is the absolute temperature (K), and all other variables are defined as before. The values of $\Delta S°$ and $\Delta H°$ for the MPSD were determined by the intercept and the slope of the fitted straight line to the plot $\mathrm{Log}\left(1{,}000\frac{q_e}{C_e}\right)$ vs. $1/T$, respectively [37].

2.4.8. Effect of competing anions on nitrate adsorption by MPSD

The anions such as chloride (Cl^-), phosphate (PO_4^{-3}), bicarbonate (HCO_3^{-1}), and sulfate (SO_4^{-2}) are commonly found in nitrate-contaminated water resources. These anions may compete with nitrate anion for adsorption sites and influence the efficiency of nitrate removal [8]. Therefore, the influence of these competing anions was evaluated by adding different concentrations of them (20, 50, and 100 mg L^{-1}) to the nitrate solution (fixed nitrate concentration of 20 mg L^{-1}) at the optimum initial pH (pH_i = 7) and adsorbent dosage (2 g L^{-1}). After stirring each sample for 30 min (equilibrium contact time), it was filtered and analyzed for residual nitrate concentration.

2.5. Desorption and reusability studies

The nitrate desorption and reusability of MPSD were investigated to shed light on the desorption and reusability properties of MPSD. To study the desorption ability, 40 mg of MPSD-loaded nitrate was stirred in NaCl-saturated solution. After 30 min, the MPSD particles were collected by filtering, dried, and eventually subjected to fresh solution. The amount of the extracted nitrate in the release medium was detected using a UV-vis spectrophotometer. To investigate the reusability of MPSD, 40 mg of MPSD was added to 20 mL nitrate solution in concentration of 20 mg L^{-1}. The mixture was stirred for 30 min at room temperature (25°C ± 1°C). The MPSD-loaded nitrate was collected by filtering. To extract nitrate, MPSD-loaded nitrate was poured into the NaCl-saturated solution and the dried MPSD was used again in the adsorption–desorption cycle for 4 times. The amount of the adsorbed nitrate in each cycle was measured by UV-vis spectra.

3. Results and discussion

3.1. Physicochemical characteristics of PSD and MPSD

The surface morphologies of PSD, MPSD, and MPSD-loaded nitrate are given in Figs. 2(a)–(c), respectively. Regarding the FESEM images, the MPSD shows a level irregularity as compared with PSD. On one hand, the modification can act as a shielding layer for PSD and rush the surface of the absorbent, which is confirmed in the relevant images. On the other hand, the MPSD had higher porosity and larger pores, which can increase the adsorption efficiency of this adsorbent. As can be seen in Fig. 2(c) compared with Fig. 2(b), the pores of MPSD decrease due to the nitrate adsorption. The EDS analyses of PSD, MPSD, and MPSD-loaded nitrate are given in Figs. 2(d)–(f), respectively. The signals of C, Si, N, and O are observed in the EDS analyses (Figs. 2(d) and (e)), which confirm the modification of PSD. Comparison of signal intensities in Figs. 2(e) and (f) confirms the correct performance of MPSD in nitrate adsorption. As can be seen, decrease in Cl signal and increase in N and O signals refer to ion exchange between chloride anion and nitrate anion in adsorption process.

Fig. 3 presents the results of elemental mapping images for MPSD. It is evident from Fig. 3 that the distribution of five elements (C, Cl, O, N, and Si) in the MPSD is uniform. In addition, the coincidence of these five elements mapping spectra confirms that they are forming a joint compound.

Fig. 4 shows graphs of nitrogen adsorption and desorption isotherm. The BET surface area analysis reveals that the MPSD has surface area value of 6.94 m^2 g^{-1}. Moreover, the average pore size of the adsorbent is about 8.2 nm.

The TGA curves of PSD and MPSD are presented in Fig. 5. As it is clear in Fig. 5, the PSD loses approximately 8% of weight at 150°C due to evaporation of moisture. There is also a significant weight loss of 55% in the range of 200°C–400°C, which may be due to the thermal degradation of the organic compound. The residual ash of PSD at about 700°C is about 8%. The TGA curve for MPSD shows four stages of weight loss. In less than 200°C, the weight loss of 10% is related to the evaporation of adsorbed moisture and solvent. Subsequently, the weight loss of 30% in the range of 200°C–300°C can be attributed to the decomposition of organic bonded molecules on the surface of PSD. Thereafter, a gradual decrease in

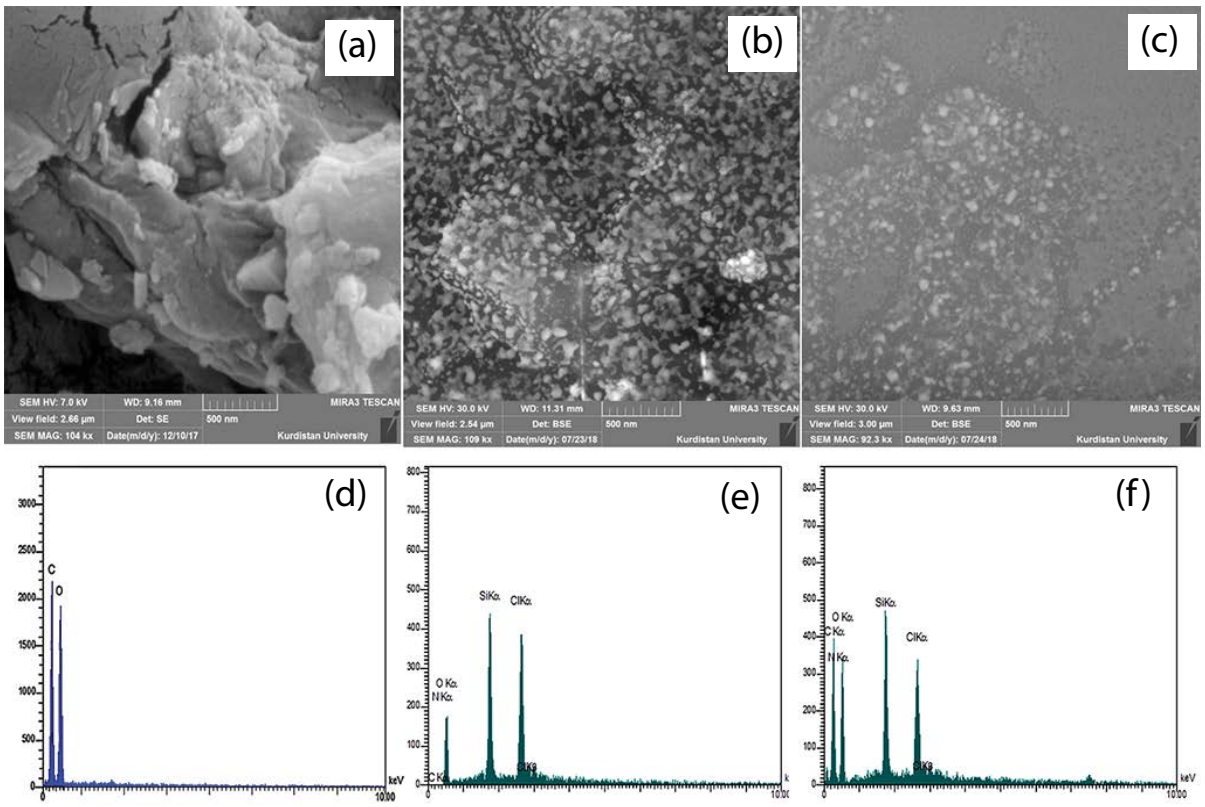

Fig. 2. FESEM images (above) and EDS curves (below) of PSD (a,d), MPSD (b,e), and MPSD-loaded nitrate (c,f).

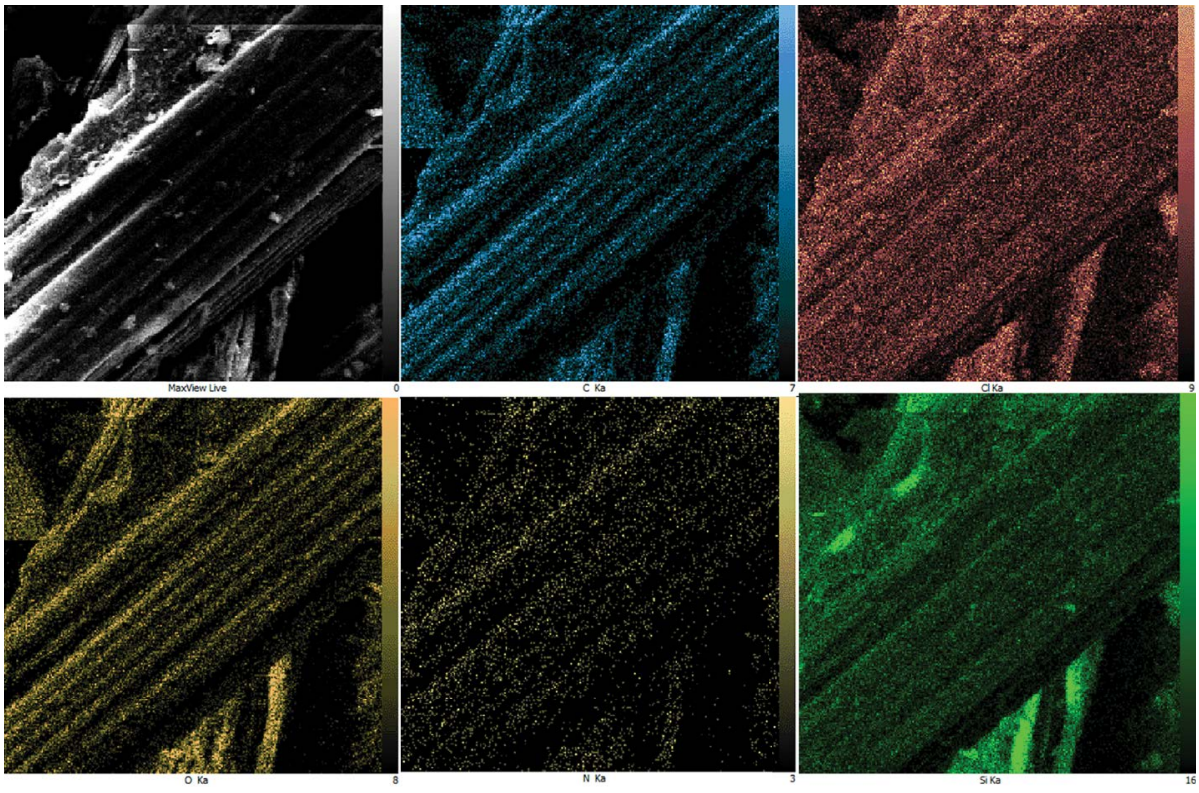

Fig. 3. FESEM elemental mapping of MPSD.

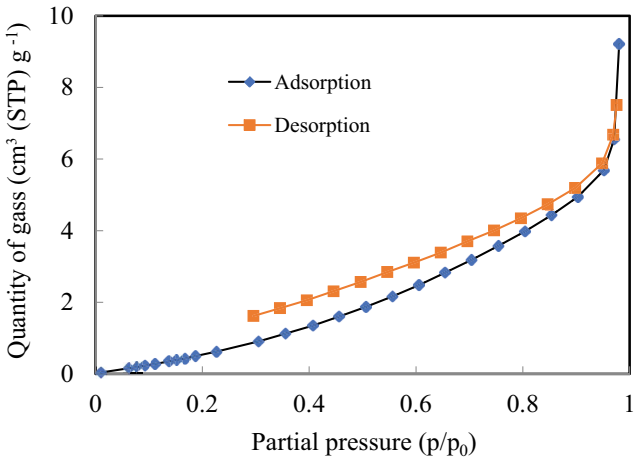

Fig. 4. BET graphs of nitrogen adsorption and desorption isotherm for MPSD.

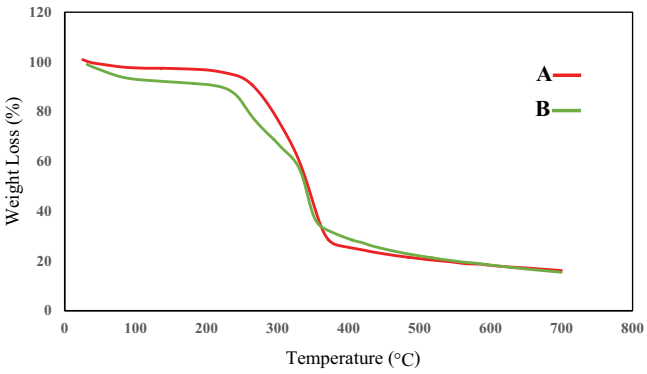

Fig. 5. TGA curves of PSD (A) and MPSD (B) under N_2 atmosphere with 10°C min^{-1} heating rate.

the weight is observed up to 600°C, which can be attributed to the loss of pendent groups in the composition and the degradation of PSD organic part. The residual ash of MPSD at 700°C was about 10%.

Fig. 6 shows the FT-IR spectra of PSD and MPSD. The FT-IR analyses of these samples illustrate the changes in functional groups. In the FT-IR spectrum of PSD, the band at 3,350–3,450 cm^{-1} is assigned to hydroxyl groups (-OH) of macromolecular association in cellulose, hemicellulose, pectin, etc. The strong adsorption band at 1,054 cm^{-1} may be due to C–O stretching. The stretching vibration at 2,950 cm^{-1} can be related to C–H bands. In the FT-IR spectrum of MPSD, the adsorption band at around 1,101 cm^{-1} corresponded to the Si–O stretching vibration. This shows that the interaction and formation of covalent bond between PSD and Dabco have been done successfully. The appearance of the new peak around 1,376 cm^{-1} is assigned to C–N stretching vibration, which is corresponded to the amine groups in the MPSD.

3.2. Effects of reaction conditions on nitrate removal by MPSD

3.2.1. Effect of initial solution pH

Fig. 7 shows the effect of initial pH of the solution on nitrate removal by MPSD. As inferred from Fig. 7, the

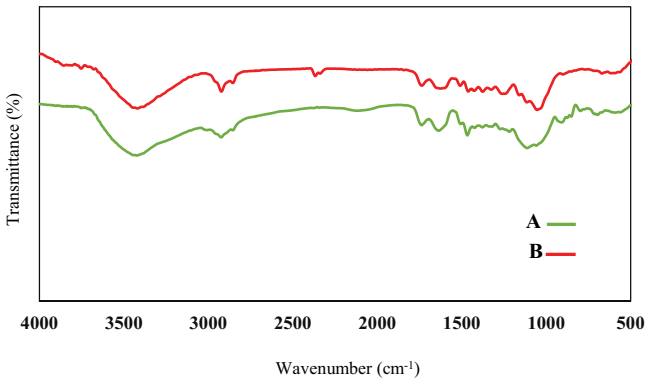

Fig. 6. FT-IR spectra of PSD (A) and MPSD (B).

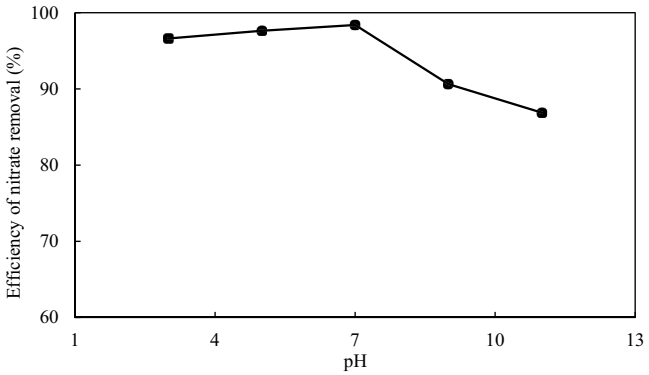

Fig. 7. Effect of initial pH of solution on nitrate removal by MPSD (Reaction conditions: V = 20 mL; C_i = 20 mg L^{-1}; T = 25°C ± 1°C; Adsorbent dosage = 2 g L^{-1}; and contact time = 120 min).

E value is almost the same for the pH values of 3–7 and slightly increases at pH 7. This implies that the MPSD is capable of removing nitrate from water in a wide range of pH, especially at neutral pH. Conversely, the E value decreases relatively rapidly when pH > 7. Several previous studies have reported similar results [8,18,43]. The decrease of E value at alkaline pH values can be attributed to increasing the negative charged sites on the MPSD and hydroxide groups. The first results in the reduction of electrostatic attraction between the NO_3^{-1} anions and the MPSD surface, and the second leads to the competition between NO_3^{-1} anions and OH^{-1} groups for the MPSD active sites [8,21,44]. It should be noted that due to relatively higher E value at pH 7, the further batch experiments were conducted at this pH.

3.2.2. Effect of contact time and adsorption kinetics

Fig. 8 presents the effect of contact time on nitrate adsorption by MPSD. As evident from Fig. 8, the adsorption capacity increases rapidly during the initial 5 min. Afterward, it increases gradually and reaches equilibrium at about 30 min. A similar behavior for nitrate removal from water by various modified lignocellulosic adsorbents has been observed in previous studies [8,26,30]. The faster adsorption of nitrate by MPSD during the initial adsorption stage can be attributed to the availability of plenty of adsorbent active sites on the MPSD surface and the slower adsorption

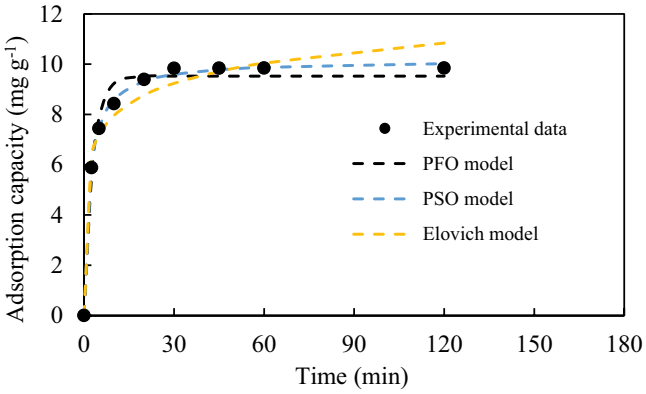

Fig. 8. Effect of contact time on nitrate adsorption capacity by MPSD and fitting the kinetic models to the experimental data (Reaction conditions: V = 20 mL; C_i = 20 mg L^{-1}; T = 25°C ± 1°C; Adsorbent dosage = 2 g L^{-1}; and pH_i = 7).

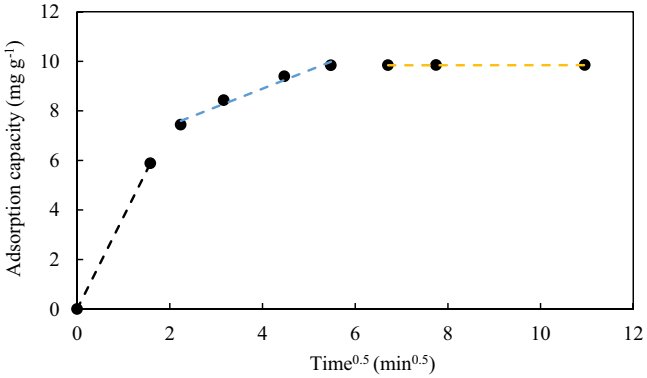

Fig. 9. IPD model for nitrate adsorption on MPSD (Reaction conditions: V = 20 mL; C_i = 20 mg L^{-1}; T = 25°C ± 1°C; Adsorbent dosage = 2 g L^{-1}; and pH_i = 7).

with further increasing time can be attributed to decrease in availability of the remaining active sites [26,37]. Considering the obtained results, a contact time of 30 min was chosen for further experiments.

As mentioned earlier, the PFO, PSO, and Elovich models were fitted with the experimental data to study the adsorption kinetics. Fig. 8 illustrates the application of kinetic models to describe the experimental data, and Table 1 presents the estimated parameters of the kinetic models and the associated values of R^2, F_{error}, and F_{error} ratio. Based on the values of R^2 and F_{error} ratio, the PSO model is found to be the best kinetic model to describe the variation of adsorption capacity with contact time. Meanwhile, the estimated q_e value of PSO model is extremely close to the experimental one. Successful fitting of the PSO model indicates that the nitrate adsorption onto the MPSD is chemisorption [45]. Also, according to the parameters of PSO model and using Eqs. (6) and (7), the values of h and $t_{1/2}$ were obtained as 5.39 mg g^{-1} min^{-1} and 1.89 min, respectively. These indicate that the adsorption of nitrate from water on the MPSD is very fast.

Fig. 9 depicts the plot of adsorption capacity versus the square root of time. As observed, this plot consists of three distinct linear regions, which demonstrates that the adsorption process occurs in three phases. Similar trends have been reported in the literature dealing with nitrate removal from water by modified lignocellulosic adsorbents [8,21,26]. The first region with the highest slope signifies a rapid external diffusion phase, which is controlled by film or surface diffusion. The second region, which has a less slope in comparison with the first region, implies a gradual adsorption stage where pore or IPD is rate-limiting. Finally, the third region, the plateau portion, represents the equilibrium or saturation stage [8,21,41]. Furthermore, Fig. 9 shows that the second region of plot of the IPD model does not pass through the origin, which implies that the IPD is not the only rate-controlling step during the gradual adsorption stage [46]. In this case, the film diffusion and the IPD take place concurrently [26,37,46].

3.2.3. Effect of adsorbent dosage

The influence of MPSD dosage on the values of E and q_e is illustrated in Fig. 10. As observed, the E value enhances with increasing the MPSD dosage up to a certain level and then takes approximately constant values as MPSD dosage further increases. Similar trends have been reported by other researches attempting to remove nitrate from water using various types of adsorbents [8,24,43]. A detailed investigation of results indicates that the E value increases from 59.27% to 91.99% as the MPSD dosage increases from 0.25 to 1 g L^{-1}, which can be attributed to the increased adsorbent surface and the increased number of the available adsorbent active sites [17,43]. However, the E value only enhances from 91.99% to 98.35% with increasing MPSD dosage from 1 to 2 g L^{-1}. This less enhancement might have been resulted from the decrease of total adsorbent surface area

Table 1
Estimated parameters of PFO, PSO, and Elovich kinetic models for nitrate adsorption on MPSD

PFO model		PSO model		Elovich model	
$q_{e,exp}$ (mg g^{-1})	9.84	$q_{e,exp}$ (mg g^{-1})	9.84	$q_{e,exp}$ (mg g^{-1})	9.84
$q_{e,model}$ (mg g^{-1})	9.52	$q_{e,model}$ (mg g^{-1})	10.17	α (mg g^{-1} min^{-1})	112.32
k_1 (min^{-1})	0.35	k_2 (g mg^{-1} min^{-1})	0.05	β (g mg^{-1})	0.86
R^2	0.99	R^2	1.00	R^2	0.99
F_{error} (%)	5.77	F_{error} (%)	1.56	F_{error} (%)	7.06
F_{error} ratio	3.70	F_{error} ratio	1.00	F_{error} ratio	4.52

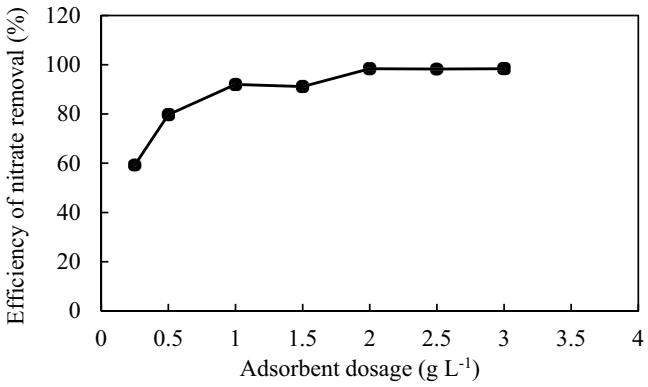

Fig. 10. Effect of adsorbent dosage on nitrate removal by MPSD (Reaction conditions: V = 20 mL; C_i = 20 mg L^{-1}; T = 25°C ± 1°C; contact time = 30 min; and pH_i = 7).

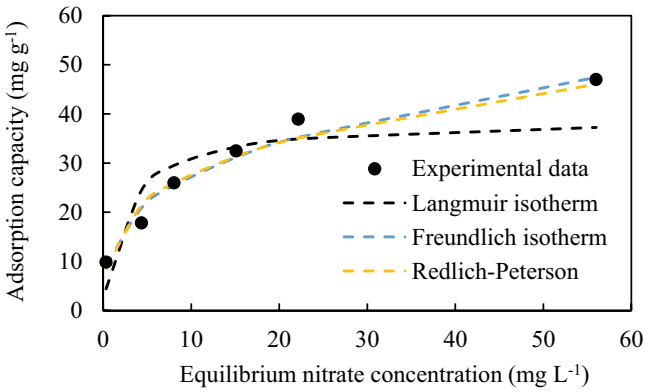

Fig. 11. Effect of initial nitrate concentration on nitrate adsorption on MPSD and fitting the equilibrium isotherms to the experimental data (Reaction conditions: V = 20 mL; T = 25°C ± 1°C; contact time = 30 min; and pH_i = 7).

and the increase of diffusional path length caused by the conglomeration of the exchanger particles at high adsorbent dosage [34,43]. It is also observed that beyond the MPSD dosage of 2 g L^{-1}, the value of E becomes almost constant and reaches the maximum value (98.35%). Therefore, the dosage of 2 g L^{-1} seems to be optimal for removing nitrate using MPSD.

3.2.4. Effect of initial nitrate concentration and adsorption isotherms

Fig. 11 illustrates the plot of the equilibrium adsorption capacity of MPSD against the initial nitrate concentration and the fitting nonlinear forms of Langmuir, Freundlich, and Redlich–Peterson isotherms to the equilibrium experimental data of nitrate adsorption on MPSD. As observed, the adsorption capacity enhances with increasing the initial nitrate concentration. The trend obtained in this study is consistent with those reported for nitrate removal from water by various adsorbents [21,24,26,47]. A detailed investigation of results shows that the q_e value increases 81.23%, 45.71%, 24.94%, 19.93%, and 20.78% with increasing C_i value from 20 to 40, 40 to 60, 60 to 80, 80 to 100, and 100 to 150 mg L^{-1}, respectively. The increase of q_e value may be due to the increase of concentration gradient between bulk and adsorbent surface, which causes better mass transfer [20]. Indeed, on one hand, the increase of initial nitrate concentration enhances the concentration gradient and provides a significant driving force to transfer nitrate anions from the bulk solution to the adsorbent surface [47,48]. On the other hand, the decrease in adsorption rate with an increase in initial concentration of nitrate can be ascribed to the less availability of adsorption active sites at higher concentration of nitrate anion [19,49]. The maximum value of q_e attained 47 mg g^{-1} in association with C_i value of 150 mg L^{-1}.

According to Fig. 11 and the corresponding values of R^2_{adj}, F_{error}, and F_{error} ratio (Table 2), the best fitting isotherm is the Freundlich isotherm followed by the Redlich–Peterson isotherm. This implies that the adsorption of nitrate on MPSD is a multilayer adsorption on heterogeneous surfaces [37,43]. Moreover, the value of n_F (3.113) indicates that the adsorption is favorable [50]. Several studies have reported the superiority of the Freundlich isotherm to describe the nitrate adsorption behavior by various adsorbents [43,44].

As can be seen in Fig. 11, the curve fitted to the equilibrium adsorption data by the Redlich–Peterson isotherm is very similar to that by the Freundlich isotherm. This is also reflected in Table 2, which shows that these isotherms give the R^2_{adj} and F_{error} ratio values close to each other. The reason for this is that the Redlich–Peterson isotherm is a hybrid isotherm incorporating features of Langmuir and Freundlich isotherms [51]. This isotherm reduces to the Freundlich isotherm when $1/K_{RP} \ll 1$ [51]. In this study, the value of $1/K_{RP}$ (7.45×10^{-3} g L^{-1}) is significantly smaller than 1, which implies that the Redlich–Peterson isotherm is more approaching the Freundlich isotherm.

Table 2
Estimated parameters of Langmuir, Freundlich, and Redlich–Peterson equilibrium isotherms for nitrate adsorption on MPSD

Langmuir isotherm		Freundlich isotherm		Redlich–Peterson isotherm	
$q_{max,}$ (mg g^{-1})	38.97	K_F (mg g^{-1} (mg L^{-1}) $^{-1/n}$)	13.02	K_{RP} (L g^{-1})	134.23
K_L (L mg^{-1})	0.39	n_F	3.11	a_{RP} (mg L^{-1})$^{-g}$	9.21
R^2_{adj}	0.65	R^2_{adj}	0.95	g	0.71
F_{error} (%)	35.88	F_{error} (%)	10.70	R^2_{adj}	0.92
F_{error} ratio	3.35	F_{error} ratio	1.00	F_{error} (%)	15.18
				F_{error} ratio	1.42

3.2.5. Effect of temperature and thermodynamic studies

The result of the temperature effect on nitrate adsorption by MPSD and the thermodynamic parameters are tabulated in Table 3. From Table 3, it is found that the equilibrium adsorption capacity decreases with increasing temperature, which means the adsorption is exothermic in nature [25]. Similar results have been detected with different adsorbents for removing nitrate from water [24,28,31]. The reasons behind the decrease in adsorption capacity at elevated temperatures may be due to increasing the mobility of the nitrate ions, damaging active binding sites of MPSD and increasing tendency to desorb nitrate ions from the solid–solution interface to the solution [52,53].

As observed in Table 3, the values of $\Delta H°$, $\Delta S°$, and $\Delta G°$ are negative. The negative value of $\Delta H°$ confirms the exothermic nature of the adsorption process [53]. The exothermic adsorption of nitrate by various adsorbents has also been reported in previous studies [8,18,21,43]. The negative value of $\Delta S°$ implies a decrease in the degree of freedom at the solid–solution interface during the adsorption process, reflecting the decreased randomness at solid–solution interface and nitrate affinity to MPSD [23]. Previous researchers reported a similar behavior for nitrate adsorption on modified polystyrene resin NDQ [18] and modified granular AC [8]. The negative values obtained for $\Delta G°$ (Table 3) reveal the feasibility and spontaneous nature of the adsorption process [53], which is consistent with the previous studies [8,18,21,43]. Meanwhile, the reduction in the absolute value of $\Delta G°$ with increasing temperature demonstrates that the nitrate adsorption onto the MPSD is more favorable at lower temperature [23].

3.2.6. Effect of competing anions

Fig. 12 presents the effect of competitive anions (Cl^-, PO_4^{-3}, HCO_3^{-1}, and SO_4^{-2}) on nitrate adsorption by MPSD. As observed, all the competing anions reduce the nitrate adsorption and the magnitude of the reduction increases with increasing the concentration of competing anions. Sulfate shows the maximum effect on nitrate adsorption by MPSD, which is explained by more negative charges of sulfate in comparison with nitrate and other competing anions investigated in this study. Similar results are available in the literature concerning the adverse effect of sulfate on nitrate adsorption by various adsorbents [8,18,26,44]. It is also found from Fig. 12 that phosphate has minimum effect on nitrate adsorption by MPSD. This may be due to the predominance of one-charge phosphate species ($H_2PO_4^{-1}$) at pH values of 6–7 [13,54]. The lower tendency of phosphate to compete with nitrate for adsorption site under similar conditions has been reported by numerous researchers [8,27]. A detailed investigation of results reveals that chloride and bicarbonate, in spite of owning one negative charge, have more inhibition effects on nitrate adsorption by MPSD in comparison with phosphate. This could have been resulted from the lower mole ratios of PO_4^{-3}/NO_3^{-1} (0.65, 1.63, and 3.26) used in this study in comparison with those of Cl^{-1}/NO_3^{-1} (1.74, 4.36, and 8.73) and HCO_3^{-1}/NO_3^{-1} (1.02, 2.54, and 5.08) [17,18]. According to the obtained results, the MPSD can remove more than 70% of nitrate from water in the presence of 100 mg L^{-1} rival anions, which demonstrates the high adsorption selectivity for nitrate.

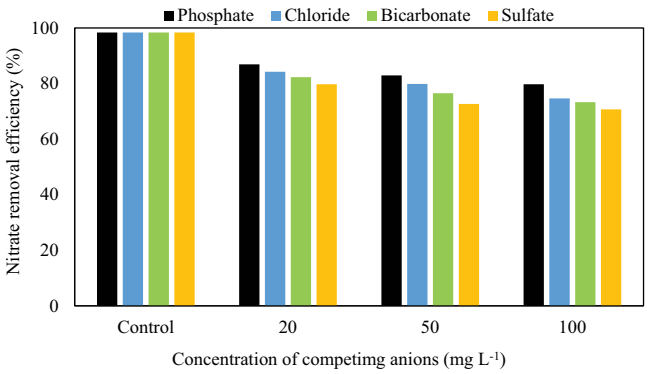

Fig. 12. Effect of competing anions on nitrate removal by MPSD (Reaction conditions: V = 20 mL; C_i = 20 mg L^{-1}; T = 25°C ± 1°C; contact time = 30 min; and pH_i = 7).

Table 3
Effect of temperature and thermodynamic parameters of nitrate adsorption on MPSD

Temperature (°C)	q_e (mg g^{-1})	$\Delta H°$ (kJ mol^{-1})	$\Delta S°$ (J K^{-1} mol^{-1})	$\Delta G°$ (kJ mol^{-1})
25	9.83	−125.83	−338.31	−24.96
35	8.49			−21.58
45	7.14			−18.19

3.3. Desorption and reusability of MPSD

To identify the desorption ability of MPSD, the release and reusability of MPSD were tested. To this end, the MPSD-containing nitrate was washed with NaCl-saturated solution for 30 min. The results showed that the total amount of adsorbed nitrate was extracted at the first extraction and there was no nitrate in the MPSD after the second and third extractions. Thus, the MPSD showed good release ability. To understand the reusability ability of MPSD, this ability was examined after four times reuse. This means that, after each adsorption, the MPSD was used for one more time until 4 times. The results showed that the ability of MPSD was 98% after four desorption–adsorption cycles (Fig. 13).

3.4. Comparative analysis

There is a huge body of literature about nitrate removal from water by various adsorbents. Application of an adsorbent to remove nitrate depends strongly on the optimum conditions of adsorption including the values of solution pH, contact time, adsorbent dosage, and the effect of rival anions. The best adsorbent is one that does not require to adjust pH, needs the least contact time and adsorbent dosage, and is not significantly influenced by the rival anions. Furthermore, the adsorbent or modifying chemical material must be nontoxic or less hazardous. In this subsection, a comparison was made based on the optimum conditions of nitrate adsorption by MPSD to situate the novel lignocellulosic adsorbent (MPSD)

Table 4
Comparison of optimum conditions for nitrate adsorption on various adsorbents

Adsorbent	E (%)	q_m^1 (mg g^{-1})	Optimum conditions of adsorption			E'^2 (%)	Reference
			pH_i	Contact time (min)	Adsorbent dosage (g L^{-1})		
Chitosan hydrogel beads	–	92.10	3	~400	–	–	[52]
Modified rice husk	94.30	~25.96	7	90	4	~69.30	[43]
Modified PB	–	180.42	6	~30	1.5	–	[21]
Modified biochar of sugarcane bagasse	~70	~24	3	60	2	–	[26]
Amine-grafted corn cob	–	~49.90	6.50	–	1	~0	[27]
Amine-grafted coconut copra	–	~55	6.50	–	1	~0	[27]
Modified pine sawdust	Over 80	133.3	3–10	~10	6	16	[24]
Modified granular AC	~80	~19.60	7	120	4	–	[8]
MPSD	98.35	47	7	30	2	70.71	This study

Dashes represent "not available".
q_m^1 represents the maximum experimental adsorption capacity.
E'^2 represents the efficiency of removal in the presence of the most competing anion.

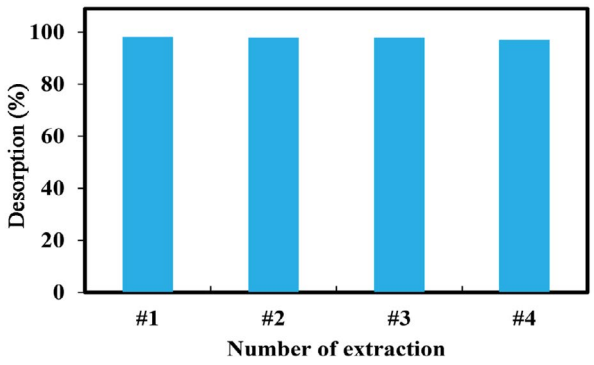

Fig. 13. Reusability of MPSD.

among those used to remove nitrate from water. Table 4 summarizes the optimum conditions for nitrate adsorption on MPSD and different adsorbents mentioned in the literature. To have a better understanding of MPSD performance, the advantages and drawbacks of each adsorbent are described below with details.

Chitosan hydrogel beads [52] and modified biochar of sugarcane bagasse [26] have the high adsorption capacity and removal efficiency of nitrate, respectively, but they require the long contact times (400 and 60 min), and their performances depend on the initial pH value of the solution. Notwithstanding modified rice husk [43] and modified granular AC [8] own high removal efficiencies, they suffer from the long contact time and high adsorbent dosage. In the case of amine-grafted corn cob [27], amine-grafted coconut copra [27], and modified pine sawdust [24], it is observed that they can well remove nitrate from water, but the presence of competing anions significantly decreases their removal efficiencies. Although modified PB [21] appears to be an efficient adsorbent for removing nitrate, the effect of competing anions is not reported (Table 4). Hence, to make a true judgement, it is necessary to examine the effect of competing anions on nitrate removal efficiency by it. Compared with other adsorbents mentioned in Table 4, the adsorbent used in this study (MPSD) has the most suitable optimum conditions for nitrate adsorption and the environmental factors have lower effects on its performance. In addition, the chemical materials used in this study to modify the PSD are less hazardous, whereas epichlorohydrin used to modify the rice husk [43], the biochar of sugarcane bagasse [26], corn cob and coconut copra [27], and pine sawdust [24] is highly toxic [28].

4. Conclusion

This study is the first attempt to remove nitrate from water using PSD chemically modified with silane group. According to the obtained results, the MPSD could remove 98.35% of nitrate from water under optimum reaction conditions (C_i = 20 mg L^{-1}; pH_i = 7; T = 25°C ± 1°C; adsorbent dosage = 2 g L^{-1}, and contact time = 30 min). The kinetic studies showed that nitrate adsorption process on MPSD was a three-step process and the PSO model fitted well with the experimental data. The Freundlich isotherm described well the adsorption equilibrium data, which demonstrated the nitrate adsorption on MPSD occurred in multilayer on heterogeneous surfaces. The obtained values of thermodynamic parameters revealed the spontaneous and exothermic nature of the adsorption process. The presence of competing anions reduced the nitrate adsorption in the order of sulfate > bicarbonate > chloride > phosphate. However, over 70% nitrate removal was still obtained in the presence of sulfate ion with concentration of 100 mg L^{-1}. Based on the obtained results, it can be finally concluded that the MPSD is a worthy candidate for efficient removal of nitrate from water. In addition, the MPSD could potentially be applied to remove other anions from water, which could be the subject of future studies.

Acknowledgement

The authors would like to express their gratitude to University of Kurdistan (UOK), Sanandaj, Iran, for financial support.

References

[1] J. Meng, S. Hong, T. Wang, Q. Li, S.J. Yoon, Y. Lu, J.P. Giesy, J.S. Khim, Traditional and new POPs in environments along the Bohai and Yellow Seas: an overview of China and South Korea, Chemosphere, 169 (2017) 503–515.

[2] E.J. Muturi, J.L. Ramirez, A.P. Rooney, C. Dunlap, Association between fertilizer-mediated changes in microbial communities and Aedes albopictus growth and survival, Acta Trop., 164 (2016) 54–63.

[3] G. Sharma, Mu. Naushad, D. Pathania, A. Kumar, A multifunctional nanocomposite pectin thorium(IV) tungstomolybdate for heavy metal separation and photoremediation of malachite green, Desal. Wat. Treat., 57 (2016) 19443–19455.

[4] Y. Ren, Y. Ye, J. Zhu, K. Hu, Y. Wang, Characterization and evaluation of a macroporous anion exchange resin for nitrate removal from drinking water, Desal. Wat. Treat., 57 (2016) 17430–17439.

[5] A. Sowmya, S. Meenakshi, Removal of nitrate and phosphate anions from aqueous solutions using strong base anion exchange resin, Desal. Wat. Treat., 51 (2013) 7145–7156.

[6] S. Sepehri, M. Heidarpour, J. Abedi-Koupai, Nitrate removal from aqueous solution using natural zeolite-supported zero-valent iron nanoparticles, Soil Water Res., 9 (2014) 224–232.

[7] T. Turki, S. Ben Hamouda, R. Hamdi, M. Ben Amor, Nitrates removal on Purolite A520E resin: kinetic and thermodynamic studies, Desal. Wat. Treat., 41 (2012) 1–8.

[8] M. Mazarji, B. Aminzadeh, M. Baghdadi, A. Bhatnagar, Removal of nitrate from aqueous solution using modified granular activated carbon, J. Mol. Liq., 233 (2017) 139–148.

[9] WHO, Guidelines for drinking-water quality, 4th edition, World Health Organization, Geneva, 2011.

[10] H. Zhang, J. Jiang, M. Li, F. Yan, C. Gong, Q. Wang, Biological nitrate removal using a food waste-derived carbon source in synthetic wastewater and real sewage, J. Environ. Manage., 166 (2016) 407–413.

[11] Y.-H. Kim, E.-D. Hwang, W.S. Shin, J.-H. Choi, T.W. Ha, S.J. Choi, Treatments of stainless steel wastewater containing a high concentration of nitrate using reverse osmosis and nanomembranes, Desalination, 202 (2007) 286–292.

[12] J. Bi, C. Peng, H. Xu, A.-S. Ahmad, Removal of nitrate from groundwater using the technology of electrodialysis and electrodeionization, Desal. Wat. Treat., 34 (2011) 394–401.

[13] P. Loganathan, S. Vigneswaran, J. Kandasamy, Enhanced removal of nitrate from water using surface modification of adsorbents—a review, J. Environ. Manage., 131 (2013) 363–374.

[14] F.S. Fateminia, C. Falamaki, Zero valent nano-sized iron/clinoptilolite modified with zero valent copper for reductive nitrate removal, Process Saf. Environ., 91 (2013) 304–310.

[15] G. Sharma, Mu. Naushad, A. Kumar, S. Rana, S. Sharma, A. Bhatnagar, F.J. Stadler, A.A. Ghfar, M.R. Khan, Efficient removal of coomassie brilliant blue R-250 dye using starch/poly(alginic acid-cl-acrylamide) nanohydrogel, Process Saf. Environ., 109 (2017) 301–310.

[16] G. Sharma, A. Kumar, Mu. Naushad, A. Kumar, A.H. Al-Muhtaseb, P. Dhiman, A.A. Ghfar, F.J. Stadler, M.R. Khan, Photoremediation of toxic dye from aqueous environment using monometallic and bimetallic quantum dots based nanocomposites, J. Clean. Prod., 172 (2018) 2919–2930.

[17] M. Kalaruban, P. Loganathan, W.G. Shim, J. Kandasamy, G. Naidu, T.V. Nguyen, S. Vigneswaran, Removing nitrate from water using iron-modified Dowex 21K XLT ion exchange resin: batch and fluidised-bed adsorption studies, Sep. Purif. Technol., 158 (2016) 62–70.

[18] Y. Wu, Y. Wang, J. Wang, S. Xu, L. Yu, C. Philippe, T. Wintgens, Nitrate removal from water by new polymeric adsorbent modified with amino and quaternary ammonium groups: batch and column adsorption study, J. Taiwan Inst. Chem. Eng., 66 (2016) 191–199.

[19] Mu. Naushad, S. Vasudevan, G. Sharma, A. Kumar, Z.A. AL-Othman, Adsorption kinetics, isotherms, and thermodynamic studies for Hg2+ adsorption from aqueous medium using alizarin red-S-loaded amberlite IRA-400 resin, Desal. Wat. Treat., 57 (2016) 18551–18559.

[20] S.N. Milmile, J.V. Pande, S. Karmakar, A. Bansiwal, T. Chakrabarti, R.B. Biniwale, Equilibrium isotherm and kinetic modeling of the adsorption of nitrates by anion exchange Indion NSSR resin, Desalination, 276 (2011) 38–44.

[21] A. Karachalios, M. Wazne, Nitrate removal from water by quaternized pine bark using choline based ionic liquid analogue, J. Chem. Technol. Biot., 88 (2013) 664–671.

[22] U.S. Orlando, A.U. Baes, W. Nishijima, M. Okada, A new procedure to produce lignocellulosic anion exchangers from agricultural waste materials, Bioresource Technol., 83 (2002) 195–198.

[23] X. Xu, B.-Y. Gao, Q.-Y. Yue, Q.-Q. Zhong, X. Zhan, Preparation, characterization of wheat residue based anion exchangers and its utilization for the phosphate removal from aqueous solution, Carbohyd. Polym., 82 (2010) 1212–1218.

[24] A. Keränen, Water treatment by quaternized lignocellulose, Dissertation, Faculty of Technology, University of Oulu, Oulu, Finland, 2017.

[25] X. Xu, B. Gao, Y. Zhao, S. Chen, X. Tan, Q. Yue, J. Lin, Y. Wang, Nitrate removal from aqueous solution by *Arundo donax* L. reed based anion exchange resin, J. Hazard. Mater., 203–204 (2012) 86–92.

[26] L.D. Hafshejani, A. Hooshmand, A.A. Naseri, A. Soltani Mohammadi, F. Abbasi, A. Bhatnagar, Removal of nitrate from aqueous solution by modified sugarcane bagasse biochar, Ecol. Eng., 95 (2016) 101–111.

[27] M. Kalaruban, P. Loganathan, W.G. Shim, J. Kandasamy, H.H. Ngo, S. Vigneswaran, Enhanced removal of nitrate from water using amine-grafted agricultural wastes, Sci. Total Environ., 565 (2016) 503–510.

[28] I.R.H. Wolkowicz, C.M. Aronzon, C.S.P. Coll, Lethal and sublethal toxicity of the industrial chemical epichlorohydrin on *Rhinella arenarum* (Anura, Bufonidae) embryos and larvae, J. Hazard. Mater., 263 (2013) 784–791.

[29] A.P. Abbott, T.J. Bell, S. Handa, B. Stoddart, Cationic functionalisation of cellulose using a choline based ionic liquid analogue, Green Chem., 8 (2006) 784–786.

[30] A.C.A. de Lima, R.F. Nascimento, F.F. de Sousa, J.M. Filho, A.C. Oliveira, Modified coconut shell fibers: a green and economical sorbent for the removal of anions from aqueous solutions, Chem. Eng. J., 185,186 (2012) 274–284.

[31] A. Mautner, H.A. Maples, H. Sehaqui, T. Zimmermann, U.P. de Larraya, A.P. Mathew, C.Y. Lai, K. Li, A. Bismarck, Nitrate removal from water using a nanopaper ion-exchanger, Environ. Sci.: Water Res. Technol., 2 (2016) 117–124.

[32] W. Xiao, B. Yan, H. Zeng, Q. Liu, Dendrimer functionalized graphene oxide for selenium removal, Carbon, 105 (2016) 655–664.

[33] Y. Zhang, Y. Li, J. Li, L. Hu, X. Zheng, Enhanced removal of nitrate by a novel composite: nanoscale zero valent iron supported on pillared clay, Chem. Eng. J., 171 (2011) 526–531.

[34] M. Sharifzadeh Baei, H. Esfandian, A. Azizzadeh Nesheli, Removal of nitrate from aqueous solutions in batch systems using activated perlite: an application of response surface methodology, ASIA-Pac. J. Chem. Eng., 11 (2016) 437–447.

[35] Y. Cebeci, Investigation of kinetics of agglomerate growth in oil agglomeration process, Fuel, 82 (2003) 1645–1651.

[36] H.N. Tran, S.-J. You, A. Hosseini-Bandegharaei, H.-P. Chao, Mistakes and inconsistencies regarding adsorption of contaminants from aqueous solutions: a critical review, Water Res., 120 (2017) 88–116.

[37] S. Dawood, T.K. Sen, Removal of anionic dye Congo red from aqueous solution by raw pine and acid-treated pine cone powder as adsorbent: equilibrium, thermodynamic, kinetics, mechanism and process design, Water Res., 46 (2012) 1933–1946.

[38] R.M.F. Bezerra, I. Fraga, A.A. Dias, Utilization of integrated Michaelis–Menten equations for enzyme inhibition diagnosis and determination of kinetic constants using Solver supplement of Microsoft Office Excel, Comput. Meth. Prog. Bio., 109 (2013) 26–31.

[39] É.C. Lima, M.A. Adebayo, F.M. Machado, In: C.P. Bergmann, F.M. Machado Eds., Carbon Nanomaterials as Adsorbents for Environmental and Biological Applications, Springer, New York, 2015, pp. 33–69.

[40] L.D.T. Prola, E. Acayanka, E.C. Lima, C.S. Umpierres, J.C.P. Vaghetti, W.O. Santos, S. Laminsi, P.T. Djifon, Comparison of Jatropha curcas shells in natural form and treated by non-thermal plasma as biosorbents for removal of Reactive Red 120 textile dye from aqueous solution, Ind. Crop. Prod., 46 (2013) 328–340.
[41] D. Ding, Y. Zhao, S. Yang, W. Shi, Z. Zhang, Z. Lei, Y. Yang, Adsorption of cesium from aqueous solution using agricultural residue-walnut shell: equilibrium, kinetic and thermodynamic modeling studies, Water Res., 47 (2013) 2563–2571.
[42] S. Dawood, T.K. Sen, Author's responses to the comment by Canzano et al and also corrigendum to "Removal of anionic dye Congo red from aqueous solution by raw pine and acid-treated pine cone powder as adsorbent: equilibrium, thermodynamic, kinetics, mechanism and process design" published in Water Research, Vol. 46, pp. 1933–1946, 2012, Water Res., 46 (2012) 4316–4317.
[43] R. Katal, M. Sharifzadeh Baei, H. Taher Rahmati, H.A. Esfandian, Kinetic, isotherm and thermodynamic study of nitrate adsorption from aqueous solution using modified rice husk, J. Ind. Eng. Chem., 18 (2012) 295–302.
[44] P.K. Singh, S. Banerjee, A.L. Srivastava, Y.C. Sharma, Kinetic and equilibrium modeling for removal of nitrate from aqueous solutions and drinking water by a potential adsorbent, hydrous bismuth oxide, RSC Adv., 5 (2015) 35365–35376.
[45] H.N. Tran, S.-J. You, H.-P. Chao, Effect of pyrolysis temperatures and times on the adsorption of cadmium onto orange peel derived biochar, Waste Manage. Res., 34 (2016) 129–138.
[46] J. Lin, Y. Zhan, Adsorption of humic acid from aqueous solution onto unmodified and surfactant-modified chitosan/zeolite composites, Chem. Eng. J., 200–202 (2012) 202–213.
[47] M. Ahmadzadeh Tofighy, T. Mohammadi, Nitrate removal from water using functionalized carbon nanotube sheets, Chem. Eng. Res. Des., 90 (2012) 1815–1822.
[48] V. Vimonses, S. Lei, B. Jin, C.W.K. Chow, C. Saint, Kinetic study and equilibrium isotherm analysis of Congo Red adsorption by clay materials, Chem. Eng. J., 148 (2009) 354–364.
[49] Mu. Naushad, G. Sharma, A. Kumar, S. Sharma, A.A. Ghfar, A. Bhatnagar, F.J. Stadler, M.R. Khan, Efficient removal of toxic phosphate anions from aqueous environment using pectin based quaternary amino anion exchanger, Int. J. Biol. Macromol., 106 (2018) 1–10.
[50] R. Chen, Q. Yang, Y. Zhong, X. Li, Y. Liu, X.-M. Li, W.-X. Du, G.-M. Zeng, Sorption of trace levels of bromate by macroporous strong base anion exchange resin: influencing factors, equilibrium isotherms and thermodynamic studies, Desalination, 344 (2014) 306–312.
[51] F.-C. Wu, B.-L. Liu, K.-T. Wu, R.-L. Tseng, A new linear form analysis of Redlich–Peterson isotherm equation for the adsorptions of dyes, Chem. Eng. J., 162 (2010) 21–27.
[52] S. Chatterjee, S.H. Woo, The removal of nitrate from aqueous solutions by chitosan hydrogel beads, J. Hazard. Mater., 164 (2009) 1012–1018.
[53] A. Bhatnagar, M. Sillanpää, A review of emerging adsorbents for nitrate removal from water, Chem. Eng. J., 168 (2011) 493–504.
[54] B. Pan, J. Wu, B. Pan, L. Lv, W. Zhang, L. Xiao, X. Wang, X. Tao, S. Zheng, Development of polymer-based nanosized hydrated ferric oxides (HFOs) for enhanced phosphate removal from waste effluents, Water Res., 43 (2009) 4421–4429.